Study of selectively buried ion-exchange glass waveguides using backside masking

Chongyang Pei (裴重阳)[1], Gencheng Wang (王根成)[1], Bing Yang (杨 冰)[1], Longzhi Yang (杨龙志)[1], Yinlei Hao (郝寅雷)[1,2], Xiaoqing Jiang (江晓清)[1,2], and Jianyi Yang (杨建义)[1,2,*]

[1]*Department of Information Science and Electronics Engineering, Zhejiang University, Hangzhou 310027, China*
[2]*Cyrus Tang Center for Sensor Materials and Applications, Zhejiang University, Hangzhou 310027, China*
**Corresponding author: yangjy@zju.edu.cn*

Received September 15, 2014; accepted November 14, 2014; posted online February 9, 2015

In this Letter, we study the characteristics of a selectively buried glass waveguide that is fabricated by the backside masking method. The results show that the surface region appears when the width of the backside mask is larger than 7 mm. Here, the glass substrate is 1.5 mm thick. It is also found that the buried depth evolution of the transition region remains almost unchanged and is independent of the width of the backside mask. The loss of the transition region is only 0.28 dB at the wavelength of 1.55 μm if the surface condition is good enough.

OCIS codes: 130.0130, 130.2755.
doi: 10.3788/COL201513.021301.

Glass is one of the essential materials in optics. The fabrication processes to realize glass waveguides can be classified into the ion-exchange process, the plasma-enhanced chemical vapor deposition process, and the femtosecond laser writing process[1,2]. The ion-exchange process, which is simple, economic, and does not require complicated manufacturing equipment, has been used to realize many devices, including optical power splitters[3], amplifiers[4], lasers[5], and optical sensors[6,7]. Among the ion-exchange glass waveguides, the selectively buried waveguides (SBWs) attract the most attention, since they provide a new method for the three-dimensional integration of optical sensors[8].

The electric field has to be partially shielded to simultaneously bring about the surface region and the buried waveguide region of the SBW during the electric-assisted ion-diffusion procedure process. Two different methods have been presented to realize this: one uses a mask on the front side[9], while the other uses a mask on the backside[10] of the glass substrate. However, the front side masking process requires the accurate control of a very small tilt angle between the waveguides and the axes of the mask to reduce the insertion loss. On the other hand, the backside masking process has a low dependency on the mask alignment and can get a low-loss transition region between the surface and buried waveguides, making it the proper method to realize the SBW. Bertoldi *et al.*[10] and Grelin *et al.*[8] used the backside masking method to actualize a Bragg grating filter and an asymmetric Y-junction, respectively. However, the characteristics of the SBWs have not been studied sufficiently. In this Letter, the buried depth and the insertion loss *IL* of the SBWs are investigated.

The sample is fabricated on a 1.5 mm-thick glass substrate by a process based on the two step ion-exchange process[3,11]. On the front side of the sample, the straight surface waveguides are fabricated first by Ag^+/Na^+ thermal exchanging. Then, on the backside, a trapezoid dielectric mask is deposited, as shown in Fig. 1. The length of the waveguide L_{SBW} is 17 mm, and the backside masked length L_{bm} varies from 3 to 12 mm. It is determined by the trapezoid mask. Therefore, the characteristics of the SBWs with different L_{bm} can be investigated using just a single sample. Finally, the electric-assisted ion-diffusion procedure is applied to achieve the SBWs.

The fabrication process flow can be divided into five steps, which are shown in Fig. 2. First, a 200 nm-thick aluminum film is deposited on the glass substrate. Then, the mask pattern of straight waveguides is transferred to the film using standard photolithography processes and chemical etching. Another 200 nm-thick aluminum film is deposited onto the backside of the wafer to prevent the Ag^+ diffusing into the backside of the glass substrate during the ion-exchange procedure. After that, the thermal Ag^+/Na^+ ion exchange is carried out at 260°C for 40 min in molten salt consisting of $NaNO_3$, $Ca(NO_3)_2$,

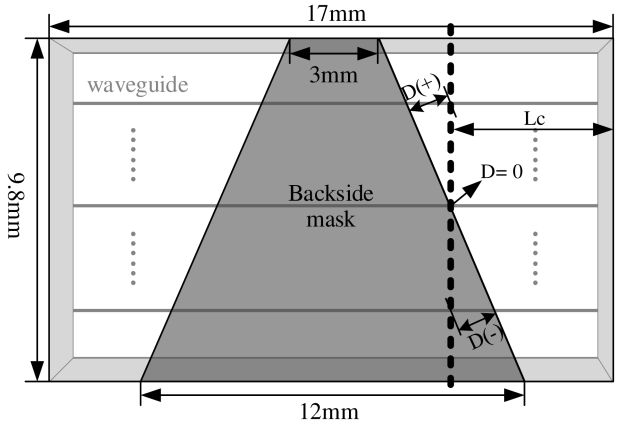

Fig. 1. Schematic of the chip, and the definition of *D*.

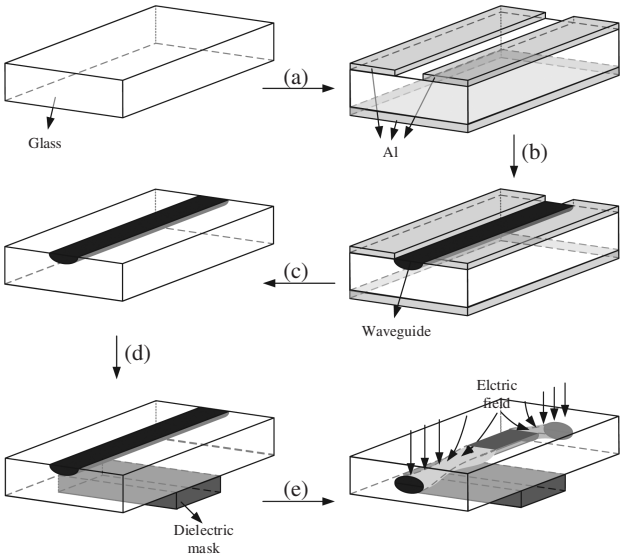

Fig. 2. Process flow for the realization of SBWs. (a) The mask deposition, photolithography process, and chemical etching and backside mask deposition. (b) The thermal Ag^+/Na^+ exchange. (c) The chemical etching of both masks. (d) The backside dielectric mask deposition. (e) The electric-assisted ion-diffusion.

and $AgNO_3$. Both aluminum films are removed using chemical etching, to prevent them from influencing the electricity involved in the electric-assisted ion-diffusion process. A trapezoid dielectric silicone rubber is then deposited onto the backside of the wafer to shield the electric field. Finally, the electric-assisted ion-diffusion process is performed for 2 h in the molten salt, which consists of $NaNO_3$ and $Ca(NO_3)_2$.

To measure the buried depth of each waveguide, the chip is cut along the dashed line, as shown in Fig. 1. It is cut at three different places, where $L_c = 5$, 7, and 8.5 mm. Here, L_c is the length from the cut end to the original end of the sample. Figure 3 shows the buried depth and some cross-section views of the waveguides at various distances, D. Specifically, D is the minimum distance from the cut end of the measured waveguide to the corresponding edge of the backside mask. D is positive when the cut end is outside of the backside mask region; inside this region, D is negative. Figure 3(a) indicates that the buried depth increases when D increases. This is because the bigger the value of D is, the greater the distance between the cut end and the edge of the backside mask region. As a result, the backside mask influences the electric field less, and the waveguide is buried deeper by the stronger electric field. Conversely, the waveguide is buried closer to the surface when the value of D is smaller, because the electric field is influenced more by the backside mask. The data are from the three cut ends of the samples, C1, C2, and C3, which correspond to $L_c = 5$, 7, and 8.5 mm, respectively, as indicated by the three insets in Fig. 3(a). It can be found that the SBW is realized successfully, and that the buried depth of the deepest waveguide in the mask region is nearly 14 μm, while that of the most superficial waveguide in the mask region is only about 2 μm.

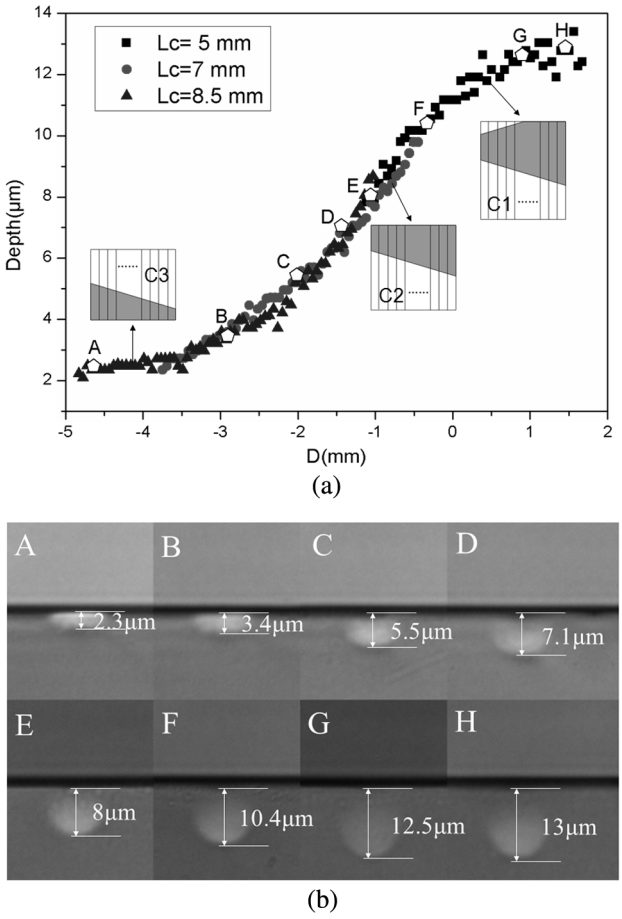

Fig. 3. (a) Buried depth. (b) The output cross-section view of the waveguides.

Figure 3(a) also shows that all of the measured data form a buried depth evolution curve, and that the buried depths are almost the same under a certain value of D, despite the fact that the data are from three different cut ends. It means that the evolution curve of the SBW is independent of $L_{\rm bm}$. Certainly, a minimum value is required. From Fig. 3(a), we can find that the transition region ranges from 1 mm outside of the backside mask region to 3.5 mm inside of the backside mask region, forming a 4.5 mm-long transition region between the surface waveguide and the buried waveguide. Based on the analysis above, it can be concluded that a minimum $L_{\rm bm}$ of 7 mm is needed to form a complete SBW, which means that the surface waveguide region does not exist until $L_{\rm bm}$ is greater than 7 mm.

Based on the above conclusion, the waveguides in the sample can be classified into incomplete and complete SBWs. The incomplete SBWs contain the buried region and the incomplete transition region. The IL of the incomplete SBWs can be written as the following equation:

$$IL = L_{\rm bw}\alpha + 2\theta + 2\varepsilon, \tag{1}$$

where $L_{\rm bw}$ represents the length of the buried waveguide, α represents its propagation loss per unit length, and θ and ε

represent the propagation loss of the transition region and the coupling loss between the buried waveguide and the standard single-mode fiber, respectively.

The complete SBWs can be classified into three regions: the buried region, the transition region, and the surface region, as shown in Fig. 4. Therefore, the *IL* of the waveguide can be written as the following equation:

$$IL = L_{\mathrm{bw}}\alpha + L_{\mathrm{sw}}\beta + 2\theta + 2\varepsilon, \tag{2}$$

where L_{sw} represents the length of the surface waveguide, and β represents its propagation loss per unit length.

From the analysis of the transition region, L_{bw} and L_{sw} have the following expressions:

$$L_{\mathrm{bw}} = L_{\mathrm{SBW}} - L_{\mathrm{bm}} - 2 \times 1 = L_{\mathrm{SBW}} - L_{\mathrm{bm}} - 2, \tag{3}$$

$$L_{\mathrm{sw}} = L_{\mathrm{bm}} - 2 \times 3.5 = L_{\mathrm{bm}} - 7. \tag{4}$$

Then, the *IL* can be obtained using the following equation:

$$IL = \begin{cases} -\alpha L_{\mathrm{bm}} + (15\alpha + 2\theta + 2\varepsilon) & 3 \le L_{\mathrm{bm}} < 7, \\ (\beta - \alpha)L_{\mathrm{bm}} + (15\alpha - 7\beta + 2\theta + 2\varepsilon) & 7 \le L_{\mathrm{bm}} \le 12. \end{cases} \tag{5}$$

In order to evaluate the performance of the transition region, the *IL* is measured and analyzed at a wavelength of 1.55 μm. Figure 5 shows the measured *IL* of the naked and the glue-coated waveguides, as well as two typical near-field images. The glue is UV-3100, the main component of which is UV-curable, modified acrylate. The refractive index of the glue is about 1.47 at 300 K, which is lower than the index of the glass substrate. An about 10 μm-thick glue film is spin-coated onto the sample.

It can be found that the *IL* can be approximately fitted by two linear curves for each case. From the difference between the *IL* curves of the naked and the glue-coated SBWs, we can see that the latter part can play a major role. The glue-coating layer effectively protects the surface of the waveguide and so minimizes the loss introduced by the surface.

When L_{bm} is less than 7 mm, the *IL* slowly increases. In this case, the transition region is gradually formed with L_{bm}. θ changes as L_{bm} changes. Considering that α is approximately 0.04 dB/mm, and ε is approximately 0.4 dB in our experiments, it can be derived with Eq. (5) that $\theta = 0.165L_{\mathrm{bm}} - 0.415$ for the naked SBWs and $\theta = 0.04L_{\mathrm{bm}}$

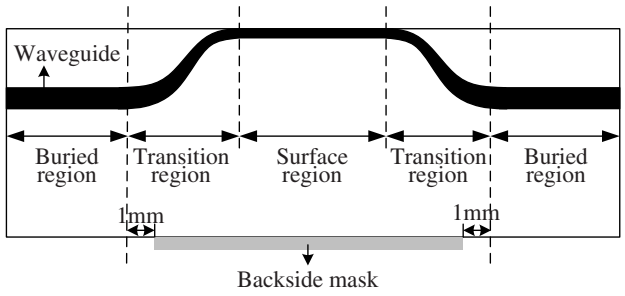

Fig. 4. The schematic of the different regions of the SBW.

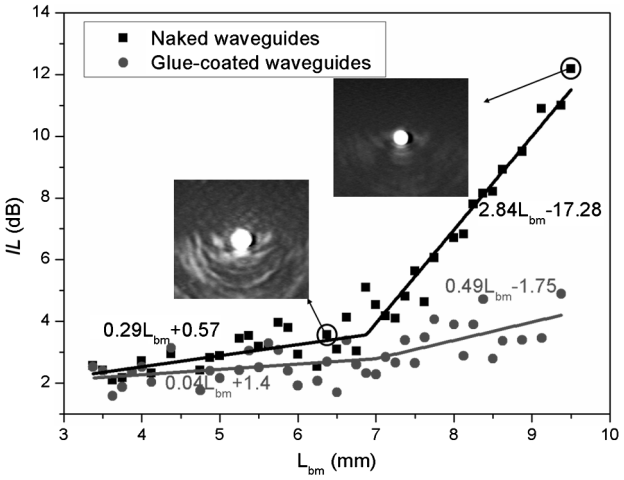

Fig. 5. The measured *IL* of the SBWs, with the different lengths of the backside mask.

for the glue-coated SBWs. The increased θ comes from two places: the transition region and the interaction with the surface.

After L_{bm} is greater than 7 mm, the *IL* is seen to increase quickly. Using Eq. (5), it can be derived that β is 2.88 dB/mm and θ is 0.74 dB for the naked SBWs, and that β is 0.53 dB/mm and θ is 0.28 dB for the glue-coated SBWs. The value of β for the naked SBWs is quite large, due to the scattering and the absorption loss caused by the nonuniformity of the surface of the sample. After the glue film is spin-coated onto the sample, the losses of the surface conditions are reduced to a lower value. However, the glue film will introduce an absorption loss to the values of β and θ. If the influence of the surface and the glue is completely removed, the propagation loss of the transition region will be further reduced.

In conclusion, the SBWs are fabricated using a backside dielectric mask during the electric-assisted ion-diffusion procedure. Then, the buried depth and the insertion loss of the SBWs are measured and analyzed. The experimental results demonstrate that the surface waveguide appears when L_{bm} is greater than 7 mm for a 1.5 mm-thick glass substrate. The shape of the transition region between the buried waveguide and the surface waveguide remains almost unchanged. It only has a loss of about 0.28 dB, which can be further reduced by improving the condition of the surface.

This work is supported by the Natural Science Foundation of China under Grant Nos. 61228501 and 61475137, the National 863 Project of China under Grant No. 2012AA012203, and the Doctoral Discipline Foundation of Ministry of Education under Grant No. 20120101110054.

References

1. X. Long, J. Bai, X. Liu, W. Zhao, and G. Cheng, Chin. Opt. Lett. **11**, 102301 (2013).
2. Y. Ju, C. Liu, Y. Liao, Y. Liu, L. Zhang, Y. Shen, D. Chen, and Y. Cheng, Chin. Opt. Lett. **11**, 072201 (2013).

3. Y. Xiao, J. Yang, and M. Wang, Proc. SPIE **8416**, 84162I (2012).
4. J. M. P. Delavaux, S. Granlund, O. Mizuhara, L. D. Tzeng, D. Barbier, M. Rattay, F. Saint-Andre, and A. Kevorkian, IEEE Photon. Technol. Lett. **9**, 247 (1997).
5. S. Blaize, L. Bastard, C. Cassagnetes, G. Vitrant, and J. Broquin, Proc. SPIE **4640**, 218 (2002).
6. C. Lavers, K. Itoh, S. Wu, M. Murabayashi, I. Mauchline, G. Stewart, and T. Stout, Sens. Actuators B **69**, 85 (2000).
7. P. V. Lambeck, Sens. Actuators B **8**, 103 (1992).
8. J. Grelin, E. Ghibaudo, and J.-E. Broquin, Mater. Sci. Eng. B **149**, 185 (2008).
9. F. Rehouma, D. Persegol, and A. Kevorkian, Sens. Actuators B **29**, 406 (1995).
10. O. Bertoldi, J.-E. Broquin, G. Vitrant, V. Collomb, M. Trouillon, and V. Minier, Proc. SPIE **5451**, 182 (2004).
11. Weiwei Zheng, Bing Yang, Yinlei Hao, M. Wang, X. Jiang, and J. Yang, Opt. Eng. **50**, 094602 (2011).